Biosensors and Bioelectronics 85 (2016) 232–239

Contents lists available at ScienceDirect

Biosensors and Bioelectronics

journal homepage: www.elsevier.com/locate/bios

Disposable self-support paper-based multi-anode microbial fuel cell (PMMFC) integrated with power management system (PMS) as the real time "shock" biosensor for wastewater

Zhiheng Xu [a], Yucheng Liu [b], Isaiah Williams [a], Yan Li [a], Fengyu Qian [c], Hui Zhang [a], Dingyi Cai [a], Lei Wang [c], Baikun Li [a,*]

[a] Department of Civil & Environmental Engineering, University of Connecticut, Storrs, CT 06269, United States
[b] College of Chemistry and Chemical Engineering, Southwest Petroleum University, China
[c] Department of Electrical & Computer Engineering, University of Connecticut, Storrs, CT 06269, United States

ARTICLE INFO

Article history:
Received 9 April 2016
Received in revised form
3 May 2016
Accepted 5 May 2016
Available online 6 May 2016

Keywords:
Microbial fuel cell
Multi-anode
Filter paper
Shock biosensor
Power management system
Power output

ABSTRACT

A paper-based multi-anode microbial fuel cell (PMMFC) integrated with power management system (PMS) was developed as a disposable self-support real-time "shock" biosensor for wastewater. PMMFCs were examined at three types of shocks (chromium, hypochlorite and acetate) in a batch-mode chamber, and exhibited various responses to shock types and concentrations. The power output of PMMFC sensor was four times as the carbon cloth (CC)-based MFCs, indicating the advantage of paper-based anode for bacterial adhesion. The power output was more sensitive than the voltage output under shocks, and thus preventing the false signals. The simulation of power harvest using PMS indicated that PMMFC could accomplish more frequent data transmission than single-anode MFCs (PSMFC) and CC anode MFCs (CCMMFC), making the self-support wastewater monitor and data transmission possible. Compared with traditional MFC sensors, PMMFCs integrated with PMS exhibit the distinct advantages of tight paper-packed structure, short acclimation period, high power output, and high sensitivity to a wide range of shocks, posing a great potential as "disposable self-support shock sensor" for real time in situ monitoring of wastewater quality.

1. Introduction

Shocks in wastewater incurred by the discharge of acutely high concentration of contaminants (e.g. organic compounds and/or heavy metals in tens or even thousands times as normal concentrations) during a short period disturb the stability of wastewater treatment plants (WWTPs) and sometimes even cause irreversible impairment of operational systems. Real-time wastewater monitor with low power requirement and high sensitivity for a broad range of shocks is critical to provide effective precaution strategies and minimize shock impacts (Liu et al., 2014; Xu et al., 2015). Installing a complete spectrum of sensors specific to each type of shock is impossible for WWTPs. Instead, developing sensors capable of real-time screening the presence/absence of a broad range of shocks is an effective solution, especially if the sensors can be self-supported for data transmission.

Microbial fuel cell (MFC), a bioelectrochemical system (BES) converting wastewater to electric energy by the microorganisms intrinsic in wastewater possesses the unique feature as wastewater shock sensor, since the jump or drop of the voltage/power output of a MFC is directly associated with electrogenic bacterial activity (Kim et al., 2007; Liu and Logan, 2004; Liu et al., 2005; Logan, 2009; Mukherjee et al., 2013; Oh and Logan, 2005; Tian et al., 2015; Wang et al., 2013) and affected by shocks in wastewater. Moreover, unlike conventional wastewater biosensors requiring coated enzymes and/or pure bacterial cells and external power supply (Curtis et al., 2009; Okochi et al., 2004; Woznica et al., 2010. Zhang et al., 2012; Zhou, 2015; Zhou and Wang, 2012), MFCs produce electric energy from wastewater and are expected to achieve self-sustained monitoring, recording, and data transmission, which substantially simplify the device setup and prolong the lifetime. Previous studies had found the good sensitivity of MFCs to toxic metal shocks and good recovery from shocks (Chang et al., 2005; Kumlanghan et al., 2007; Li et al., 2014; Liu et al., 2014; Wang et al., 2014; Xu et al., 2015). However, there are three main challenges of MFC shock sensors. First, the acclimation time of traditional MFCs (e.g. tubular bioreactor, single chamber, and

* Corresponding author.
E-mail address: baikun@engr.uconn.edu (B. Li).

http://dx.doi.org/10.1016/j.bios.2016.05.018
0956-5663/

carbon cloth-based anode) is pretty long (3–15 days, Chang et al., 2005; Kumlanghan et al., 2007; Li et al., 2014; Liu et al., 2014; Wang et al., 2014), making it impossible for real-time shock monitoring and prompt recovery of signals after shock. A novel membrane-based MFC sensor was developed using hydrophilic microporous filter membrane to shorten the acclimation period to 2–3 h (Fraiwan et al., 2013; Nguyen et al., 2014; Xu et al., 2015). But filter membrane is awfully fragile and expensive for "disposable" application in wastewater systems. MFCs with anode paper reservoirs were fabricated to accelerate bacterial growth and maintain bacterial activity (Fraiwan et al., 2013; Nguyen et al., 2014), but the requirement of constant bacterial injection to reservoirs and the bulky structure of MFC-reservoir posed high difficulty for installment in WWTPs. Second, the voltage output of single-anode MFCs has been used as the signal (Liu et al., 2014; Logan, 2009; Oh and Logan, 2005; Xu et al., 2015). However, the difference between the stable output before shock and the output after shock was too small ($\leq$ 0.15 V, Liu et al., 2014; Xu et al., 2015) due to the limited voltage output of MFCs (Liu and Logan, 2004). This minuscule response causes a potential fault warning and lowers sensitivity. One approach to enhance the response is to increase the voltage output by connecting multi-anode in series, with the precondition that each anode should be isolated into separate media units (Aelterman et al., 2006). But for a MFC sensor being inserted in wastewater with all anodes sharing the same media (wastewater), it is impossible to achieve the isolated multi-anode in series, and thus unable to increase the voltage output of a MFC sensor. Third, the power output of MFC with single pair electrode is still low (0.08 mW (Liu et al., 2014; Xu et al., 2015), which is insufficient to support the data recording and transmission (normally need 10–2000 mW (Donovan et al., 2008, 2011; Shantaram et al., 2005).

The objective of this study is to develop Paper-based Multi-anode Microbial Fuel Cell (terms as PMMFC) integrated with power management system (PMS) as a disposable self-support (meaning it functions (e.g. monitoring and data transmission) without the need of external power supply) "shock" sensor for real time in situ monitoring of wastewater quality. The breakthrough lies in enlarging and harvesting power output of PMMFC through parallel connection and PMS, and using power output instead of voltage output as the MFC signal, which is expected to enhance the sensitivity and minimize the false warning of shocks. This study consisted of three tasks. First, the acclimation and power output of PMMFC was examined and compared with the paper-based single-anode MFC (termed as PSMFC) and the traditional carbon cloth-based multi-anode MFC (CCMMFC) to determine the advantage of multi-anode configuration and filter paper anode. Second, the frequency of data transmission in PMMFC, PSMFC and CCMMFC was simulated to explore the possibility of long-term self-sustained sensing. Third, three types of shocks were examined with chromium (Cr^{6+}) as the toxic metal, sodium hypochlorous (NaClO) as the disinfectant, and sodium acetate (NaAc) as the organic contaminant in wastewater. The sensitivity of power output and voltage output was compared at different shock types and concentrations. Power outputs of PMMFCs before and after shocks was validated using regression statistical analysis.

2. Materials and methods

2.1. Fabrication of PMMFCs

The PMMFC consisted of 4 anodes (5 cm $\times$ 5 cm) and 1 cathode (3 cm $\times$ 3 cm). Multi-anode was used to enhance power output compared with single anode MFC. Filter paper has the similar feature (hydrophilic and microporous) as filter membrane, but is less expensive and more mechanic durable than filter membrane, as demonstrated in previous study (Xu et al., 2015). Anodes were made by coating carbon ink (Microcircuit Material, DuPont) (thickness: $<$1 mm) on both sides of a filter paper (P8, Fisher Science) (Fig. 1(a)). The filter paper was then folded to form four blocks as four individual anodes with each anode being connected to an external resistance (R_{ext}: 480 Ω) (Fig. 1(b)). Cathode was made by coating 4-layer polytetrafluoroethylene (PTFE) on carbon cloth facing air and the Platinum-loaded side (Pt: 0.5 mg cm^{-2}) facing wastewater (Oh et al., 2004). After assembly, the PMMFC was inserted into a batch-mode container (Fig. 1(c)).

Before the shock tests, PMMFC was acclimated in wastewater taken from the influent of the University of Connecticut Wastewater Treatment Plant (chemical oxygen demand (COD): 250–350 mg L^{-1}). The voltage outputs across four R_{ext} connected with four anodes were recorded using a data logging system (Keithly 2700). The power outputs were calculated based on Eq. (1).

$$P = \sum_i V^2/R_{ext} \quad (1)$$

where V is the voltage across the R_{ext} (mV), R_{ext} is the external resistance (Ω), i refers the number (1, 2, 3 and 4) of external circuits.

The PMMFC with 4-anode/1 cathode was compared with two control MFCs (anode area: 5 cm $\times$ 5 cm). The first one was a paper-based single-anode MFC (termed as PSMFC) to determine the enhancement of multi-anode. The second one was a carbon cloth (CC)-based multi-anode MFC (termed as CCMMFC) with the same configuration (4-anode/1 cathode) to elucidate the effect of anode materials on power output. Specifically, the anode of the PSMFC was the single filter paper coated with carbon powder. The anode of the CCMMFC was made by folding CC (Fuel Cell Earth LLC, MA) into four pieces anodes (Fig. 1(b)). The cathodes were the same as that in the PMMFC.

2.2. Internal resistance (R_{in}) of the MFCs

The power density curve was acquired by recording the voltages over a series of R_{ext} (36–21090 Ω) of MFCs (PMMFC, PSMFC and CCMMFC) using a digital multimeter. The polarization curves recorded the power density as a function of current density, which were calculated according to Eq. (2) and Eq. (3).

$$Power\ \ Density = \frac{V^2}{R_{ext}k} \quad (2)$$

$$Current\ \ Density = \frac{V}{R_{ext}k} \quad (3)$$

where R_{ext} is the external resistance (Ω), V is the voltage across R_{ext} (mV), and k is the anode project area of MFCs. The internal resistance (R_{in}) was determined based on the maximum value on the polarization curve. The R_{in} measurement was duplicated three times.

2.3. Simulation of MFCs integrated with power management system (PMS)

The power outputs of PMMFC, PSMFC and CCMMFC were simulated individually to determine the final power output available for data transmission at a duration of 60 mins when integrated with a charge pump-based power manager system (termed as PMS, power requirement: 1.2 mW). The major components of a PMS (Fig. S1) were a multi-anode decoupling circuit, a charge pump, a super capacitor, a reference voltage, a voltage controlled oscillating, a switch, and a DC–DC converter (Droppo et al., 2003).

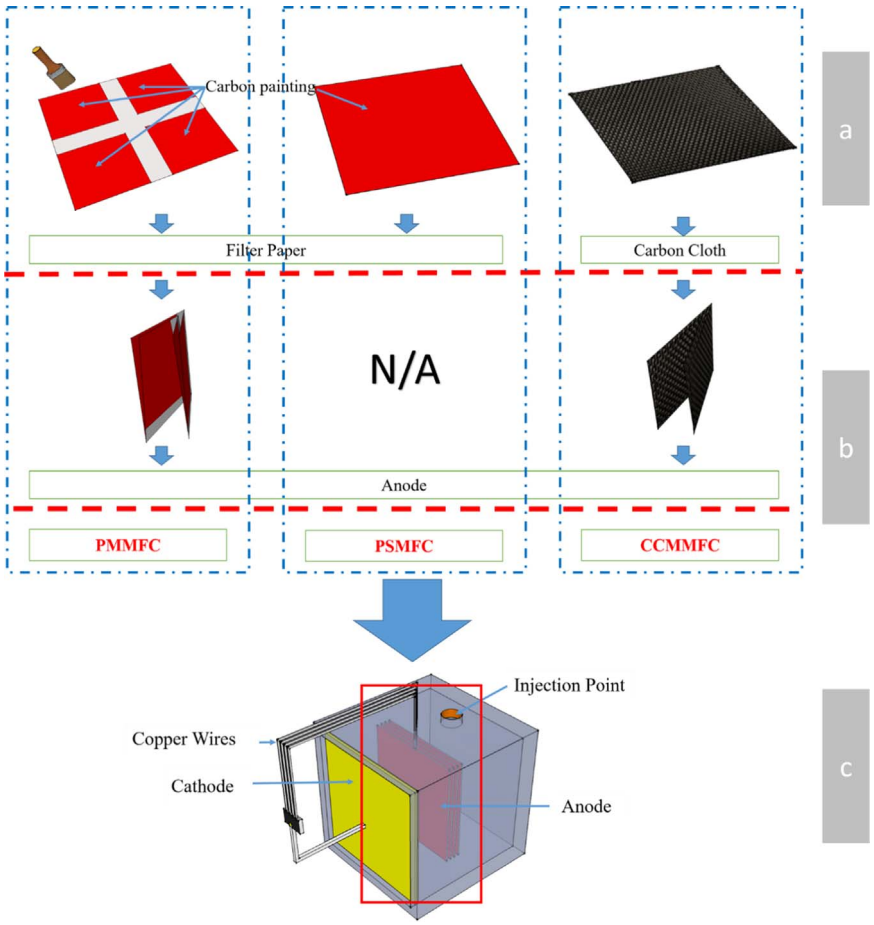

Fig. 1. The fabrication process of MFC sensors. (a: anode types: multi-anode filter paper, single-anode filter paper and multi-anode carbon cloth; b: folding anode materials to form multi-anode; c: installing a MFC sensor into a batch-mode chamber).

Following the charge pump, a super capacitor was placed to accumulate the energy from the pump discharges. The inherent efficiency of the PMS was directly dependent on the efficiency of the components (e.g. charge pumps, converter) used (Donovan et al., 2011), and was calculated according to Eq. (4).

$$\eta_{overall} = \eta_{1*}\eta_2 \quad (4)$$

where, $\eta_1$is the efficiency from the MFC to the super capacitor, and η_2 is the efficiency of the DC–DC converter. $\eta_{overall}$ was estimated as 40% based on previous studies (range: 20–60%, Donovan et al., 2011; Karra et al., 2014), mainly affected by the number of the anode. A switch unit with the voltage controlled oscillating was applied to control this energy transfer process between the super capacitor and the DC–DC converter, which enabled the energy transfer when the voltage on the super capacitor was high enough (>2 V) and disabled the energy transfer when the voltage on the super capacity dropped below a threshold (1.5 V). When the voltage of the capacitor drops from U_{max} (2 V) to U_{min} (1.5 V), a signal (e.g. the power output) was transferred and recorded by a computer terminal, so that the monitored data of MFC sensors can be recorded on a real-time mode.

2.4. Shock tests in the batch-mode container

Three types of chemical shocks (Cr^{6+}, NaClO and NaAc) were injected to the batch-mode container (Fig. 1(c)). Chromium (Cr^{6+}) is a well-known toxic metal with the limitation of 0.1 mg L^{-1} in drinking water (EPA 816-F-09-0004), and high Cr^{6+} concentration ($>$ 10–20 mg L^{-1}) occurs in wastewaters from electroplating and chrome tanning (Gupta et al., 2011; Monser and Adhoum, 2002). As one of the most classical toxic metal in wastewater, the Cr^{6+} shock was selected to examine for the sensitivity of MFC biosensors and compare with previous studies (Liu et al., 2014; Xu et al., 2015). The Cr^{6+} shocks were examined at three concentrations: 5 mg L^{-1} as the upper-end Cr concentration in wastewater, 10 mg L^{-1} and 20 mg L^{-1} as the shocks in wastewater, which was achieved by injecting 150 μL, 300 μL, and 600 μL K_2CrO_4 solution (1000 mg L^{-1} Cr^{6+}), respectively. The dilution effect was ignored since the injection volume (150–600 μL) only counted for less than 1% of the chamber volume (30 mL).

Chlorination is the routine disinfection process for water and wastewater treatment plants. The recommended concentrations of residual chlorine for disinfection are between 0.5 and 1.0 mg/L, which is well below any level known to demonstrate physiological efforts on mammals (Brungs, 1973). However, certain accident, such as free chlorine leakage could rapidly cause the spike of chlorine (over 100–1000 times as residual chlorine) in wastewater and thus becoming toxic to aquatic life. But this chlorine leakage is difficult to catch in a real time mode using routine methods (e.g. polymerase chain reaction (PCR) and electrical probe) (Kolenbrander et al., 2010; Livak and Schmittgen, 2001). The toxicity of chlorine was that low concentration hypochlorous acid exerted a rapid and selective inhibition of bacterial growth and cell division (Dukan et al., 1999; McKenna et al., 1988). Until now, chlorine shock has not been examined for MFC biosensors. Chlorine shocks were examined at three concentrations: 50 mg L^{-1} as the upper-end chlorine concentration in wastewater, 100 mg L^{-1} and 200 mg L^{-1} as the shocks in wastewater, which was achieved by

injecting 12 μL, 24 μL, and 48 μL NaClO solution (12.5% NaClO solution, Fisher Scientific), respectively.

The fluctuation of organic contaminants in wastewater has been well recognized to affect microbial activity and treatment efficiency in WWTPs (Curtis et al., 2009). Routine measurements (e.g. chemical oxygen demand COD and biological oxygen demand BOD) are off-line and *ex situ* (Jouanneau et al., 2014), which makes it impossible to real time capture organic shocks. There were two reasons for examining organic matter shocks. First, the MFC response to different organic shocks and toxic chemical shocks (e. g. Cr^{6+}, chorine) was determined. Second, organic matter shocks occurred frequently in wastewater, but were unable to be detected in real-time mode. The capability of PMMFC sensors to catch the organic shock was examined and compared with previous studies (Liu et al., 2014; Jiang et al., 2010; Santoro et al., 2011). In this study, sodium acetate (NaAc) was selected to simulate organic contaminants in wastewater. High organic substrate concentrations (e.g. 200 mg L^{-1} NaAc) had been found to affect the voltage output of MFCs (Liu et al., 2014; Jiang et al., 2010; Santoro et al., 2011). The NaAC concentration shock was selected as 200 mg L^{-1} by injecting 60 μL of concentrated NaAc solution (100 g L^{-1}) into the container. All shock tests were duplicated in three times (data not shown).

2.5. Shock significance analysis of PMMFC power outputs

Two datasets were selected from each concentration shock (Cr^{6+}, NaClO and NaAC) to evaluate the shock significance of power output and distinguish the PMMFC sensor signals from noises. One dataset was taken 120 mins before shock injection, and the other was taken during the shock period (SP) defined as the period from the shock injection to the stable power output. Statistical regression analysis of these datasets was performed using Microsoft Excel with data regression analysis. The whole analysis were duplicated in three times for the data obtained from the duplicate shock tests (data not shown).

2.6. Biofilm formation on the anode membrane

Biofilms growing on the anodes of PMMFCs and CCMMFCs after 1-month period were observed using a scanning electron microscope (SEM) (Model: Joel6335F) as previously described (Santoro et al., 2011).

3. Results and discussion

3.1. Acclimation and power output of MFC sensors

Anode materials directly affected the power output of MFC sensors when put into wastewater. The power output of the PMMFC and PSMFC sensors instantaneously stabilized at 0.33 mW and 0.08 mW, respectively, while the power output of CCMMFC was only 0.06 mW within 3 h after installation (Table S1). Because power output is associated with bacterial electrogenic activities (Liu and Logan, 2004; Liu et al., 2005; Logan, 2009), this discrepancy showed that sufficient bacteria attached to the anode filter paper (PMMFC and PSMFC) and started the electron transfer instantaneously after being exposed to wastewater. In contrast, it took traditional carbon cloth (CC) anode at least 3–15 days to acclimate bacterial growth (Chang et al., 2005; Kumlanghan et al., 2007; Li et al., 2014; Liu et al., 2014; Wang et al., 2014). Filter paper has more fine fibers and higher surface area than carbon cloth (SEM images, Fig. S2), which accelerated the biofilm formation. Previous studies found that the short acclimation time of filter membrane-based anode MFC was closely correlated with its strong absorption capacity and large surface area (Kolenbrander et al., 2010; Yang et al., 2012). The microporous filter paper (porous size: ~20 μm) used in the study exhibited the almost same characteristics as microporous filter membrane (Mixed Cellulose Ester Membranes, pore size: 0.22 μm, Millipore) (Xu et al., 2015) with fast immobilization of bacterial cells on the anode, and thus shortening the acclimation period of MFC sensors. In addition, the filter paper is stronger and much less costly than filter membrane.

The internal resistances (R_{in}) of PMMFC, PSMFC and CCMMFC were similar around 547Ω (polarization curve, Fig. 2). Previous study using the same fabrication approach of coating carbon ink on filter membrane had the R_{in} of about 1400 Ω (Xu et al., 2015). The reason for the lower R_{in} was that the coarse fiber on filter paper was much easier than filter membrane to form the "coated" carbon layer, so that the electronic conductivity enhanced on the filter paper. The power output of a MFC is directly affected by open circuit potential (OCP) and R_{in}, both being associated with electrogenic activity and system conductivity (e. g. anode, cathode, and wastewater) (Logan et al., 2006). The power output can be simply described as,

$$P=(OCP - IR_{int})^2/R_{out} \quad (5)$$

where IR_{int} is the sum of all internal losses of a MFC, I is the current (I) generated in a MFC, R_{out} is the resistance of the external circuit. For single-anode MFC, the power output with filter paper (0.08 mW, Fig. 3(a), Table S1) was almost 4 times as the one with filter membrane (0.02 mW, Liu et al., 2014) and was 1.33 times higher than the carbon cloth (CC) (0.06 mW, Fig. 3(a), Table S1).

Multi-anode configuration clearly enhanced the power output compared with single-anode. The power output of the PMMFC (0.33 mW) was 4 times as that of PSMFC (0.08 mW) based on monthly data (Fig. 3(a), Table S1), and well corresponded with the anode number (4 anodes). In addition, the power output of the PMMFC was 8 times as that of CCMMFC (0.04 mW), demonstrating the advantage of filter paper over CC. The main reason was that the blank areas between multi-anodes on low-conductive filter paper (as shown in Fig. 1(a)) prevented the short circuit on anode, while multi-anode on CC were highly electronically conductive with the resistance of less than 10 Ω and easily suffered from short circuit. Developing multi-anodes on a highly conductive CC was like forming one big anode (electronically conductive), rather than forming multiple separated small anodes on none-conductive filter paper. Previous studies verified that at the same area, the multiple separated anodes collected much more electrons than a single anode (Liu et al., 2016). This study showed that multi-anode made on the filter paper reached much higher power output than traditional conductive CC anode.

3.2. Self-sustained power generation of PMMFCs to support data transmission

Most of wastewater quality tests have been conducted off-site and caused long lag time for WWTPs to recover after shocks. The unique feature of MFC sensor integrated with power management system (PMS) is to harvest the energy from wastewater and support data transmission to achieve self-sustained real-time water quality monitoring. The initial charge time (ICT) refers to the time that PMS started charging from 0 V to U_{max} (2 V). The power outputs of PMMFC, PSMFC and CCMMFC for simulation were obtained by averaging the values through one-month operational period (Table S1). The common charge time (CCT) refers to the time that PMS charged from U_{min} to U_{max}. In the simulation of MFCs integrated with PMS (Fig. 3(b)), the ICT and CCT of a PMMFC were much shorter than PSMFC and CCMMFC. The PMMFC system transferred 28 times data per charging (60 mins in this

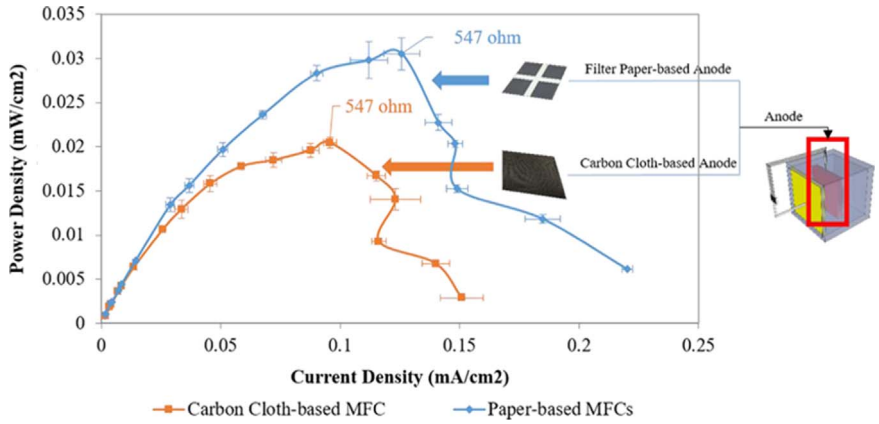

Fig. 2. Power density curves of CCMMFC and PMMFC sensors.

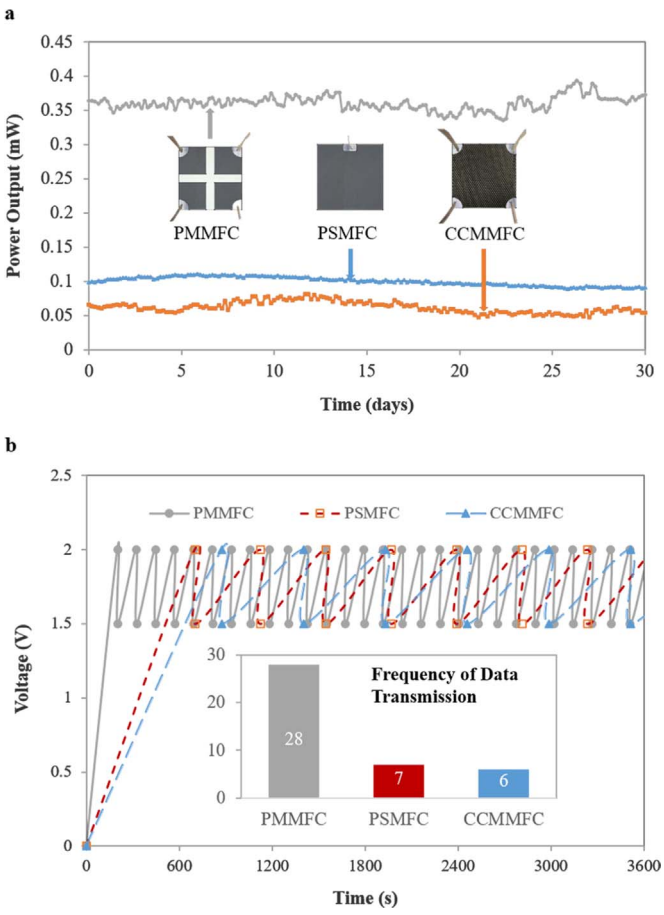

Fig. 3. Power output of the PMMFC, CCMMFC, and PSMFC during one month operational period (a) and simulation of charging cycles of the integrated MFC/PMS for data transmission within 60 min (Inset figure: The frequency number of data transmission of each type MFC sensor) (b).

simulation), which was much more frequent than PSMFC and CCMMFC (only 6–7 times), and thus enhancing the stability of real-time wastewater shock sensors. It should be noted that total power output of a PMS can be recorded using a multimeter with an integrated chip (IC) through voltage output, making real-time recording "power output" signals possible.

3.3. Sensitivity of the MFC shock sensors to Cr^{6+} Shocks

The PMMFC sensor was examined at three concentrations of Cr^{6+} shocks. The power outputs of the PMMFC sensor stabilized at 0.35 mW (based on monthly data, only 120 min are shown in Fig. 4 (a)) before the shock injection. The power output dropped to 0.08 mW 120 min after the 10 mg L^{-1} Cr^{6+} shock, and rapidly dropped to 0.01 mW 8 min after the 20 mg L^{-1} Cr^{6+} shock (Fig. 4 (a)), meaning the 35-time drop of power output within 8 min. Similar membrane-based MFC sensors exhibited the 6-time drop of voltage output within 8 min after 20 mg/L Cr^{6+} shock (Xu et al., 2015), demonstrating that the PMMFC sensor had a higher sensitivity to Cr^{6+} shock concentrations. The power output of the PMMFC recovered from 0.2 mW (the inhibition status) to 0.33 mW (the stable status) within 60–80 h after 20 mg/L Cr^{6+} shock (Fig. S3), which was similar to membrane-based MFC sensors in previous studies (Liu et al., 2014; Xu et al., 2015). The Cr^{6+}, a powerful oxidizing agent tends to be irritating and corrosive and passes through cell membranes and induces huge oxidative stress (Stohs and Bagchi, 1995). The sharp drop of the power output indicated the inhibition of electrogenic bacterial activities upon Cr^{6+} shocks, even though Cr^{6+} solutions increased wastewater ionic strength and conductivity. The duplicate test followed the same trend. The response of the CCMMFC followed the same trend as the PMMFC, but in a much mild mode (Fig. 4(a)), indicating that the PMMFC sensor could prevent the false signals.

The slope of the signal curve after 10 mg L^{-1} Cr^{6+} shock demonstrated that the power output slope (0.022) of PMMFC was about 2.5 times as the voltage output slope (0.008, Fig. 4(b)), indicating that multi-anode configuration and parallel connection could almost linearly increase the power output of MFCs and lead to an easy detection of shock signals. It should be noted that the slope of 0.022 was achieved with 4-anode, and would certainly keep increasing with more-anode (e.g. 8, 12, 20 paper-based anodes) so that the sensitivity of the MFC sensors can be further enhanced.

3.4. Sensitivity of the PMMFC shock sensors to NaClO Shocks

The power output responses of the PMMFC sensor to NaClO shocks were similar to Cr^{6+} shocks. Instead of a sharp power drop upon Cr^{6+} shock, a jump of power output was observed with the increase in NaClO concentration. The 200 mg L^{-1} NaClO shock cause a sharp power drop from 0.35 mW to 0.025 mW within 120 mins after injection (Fig. 5(a)), compared with a slow power drop after 100 mg L^{-1}(0.35 mW to 0.13 mW) and 50 mg L^{-1} NaClO (0.35 mW to 0.08 mW). Unlike the 20 mg/L Cr^{6+} as the acute toxic element inhibiting anaerobic electrogenic bacteria rapidly (Fig. 4), high concentration of HClO, the main chemical compound after the dissolution of NaClO in water induced slowly inhibit the bacteria activity. The 50 mg/L NaClO caused a steady drop of

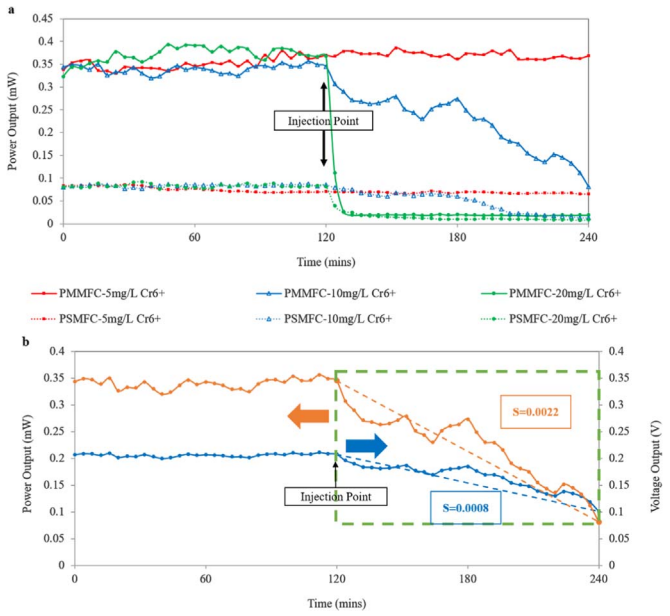

Fig. 4. Sensitivity of MFC sensors to Cr^{6+} shocks. (a: power output response of PMMFC and PSMFC sensor under 5, 10, and 20 mg L^{-1} Cr^{6+} shock; b: power output and voltage output of PMMFC sensor under 10 mg L^{-1} Cr^{6+} shock).

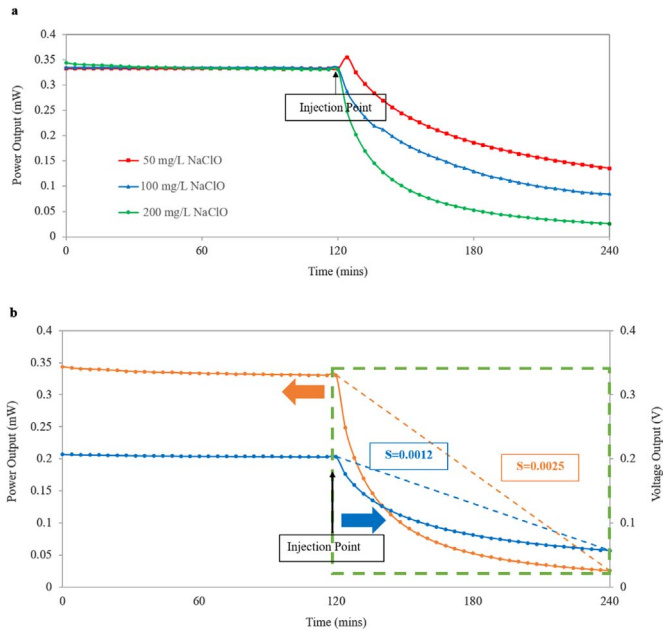

Fig. 5. Sensitivity of PMMFC sensor under NaClO shocks. (a: power output response to 50, 100, and 200 mg L^{-1} NaClO shock; b: power output and voltage output under 200 mg L^{-1} NaClO.

power output (Fig. 5(a)), which was different from a slight drop of power output caused by 5 mg/L Cr^{6+} (Fig. 4(a)), demonstrating that the NaClO concentration as low as 50 mg/L already inhibited bacterial activity and reflected by the power output drop. The slope (0.0025) of the power output signal curve after NaClO shock was about 2 times as the voltage output slope (0.0012, Fig. 5(b)), meaning a better indicator for shocks.

Interestingly, when the NaClO concentration was increased to 1200 mg/L, the power output of PMMFC sensors increased after injection (Fig. S4a), and the increment was consistent with NaClO concentration (1200–4700 mg/L). Unlike the drop of power output at NaClO concentration of 50–200 mg/L, the increase in power

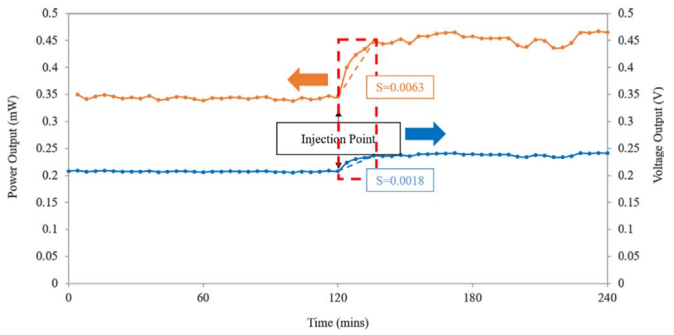

Fig. 6. Power output and voltage output responses of PMMFC sensor to 200 mg L^{-1} NaAc shock.

output at high NaClO concentration (1200–4700 mg/L) was caused by the chlorine chemical fuel cell instead of microbial activity in MFCs. NaClO higher than 2.6 mg/L was reported to inactivate bacterial cells (McKenna et al., 1988). Thus, NaClO concentration of 1200–4700 mg/L converted MFCs to chemical fuel cells with chlorine as the major reagent (Eq. (7)). The standard-state reduction potential of the cathode increased from 1.229 V (Eq. (6)) (Santoro et al., 2011) to 1.63 V (Eq. (7)) (Shiers et al., 2016), leading to a higher OCP of PMMFC sensors. HClO might react with organic matters due to this high standard-state reduction potential, leading to the conversion of PMMFC from MFC to chemical fuel cell. Moreover, high NaClO concentration substantially increased the conductivity of solution, and lowered the R_{in} of the PMMFC sensors from 547 Ω to 262 Ω (Fig. S4b). The opposite patterns under low NaClO concentration (50–200 mg/L) and high concentration (1200–4700 mg/L) clearly demonstrated that the power output of PMMFCs was directly associated with microbial activity and shock concentrations.

$$O_2(g) + 4H^+(aq) + 4e^- \rightarrow 2H_2O \qquad E = +1.229(1) \quad (6)$$

$$2\,HClO\,(aq) + 2\,H^+(aq) + 2\,e^- \rightarrow Cl_2(g) + 2\,H_2O \qquad E = +1.63\,(2) \quad (7)$$

3.5. Sensitivity of the PMMFC shock sensors to NaAc Shocks

The COD concentration of the container before the NaAc shock tests was about 250 mg/L. After sodium acetate (NaAc) shock (200 mg L^{-1}) was injected, the power sharply jumped from 0.35 mW to 0.40 mW within 4 mins and to 0.45 mW within 12 mins (Fig. 6). The voltage change, 0.2–0.25 V was similar to the change in the previous study (0.10–0.14 V, Liu et al., 2014). Previous studies found that higher organic substrate concentrations increased the voltage output of MFCs (Jiang et al., 2010; Santoro et al., 2011), mainly due to the increase in wastewater conductivity and the decrease in the R_{in} of MFCs. The slope of the signals after NaAc shock showed that power output slope (0.0063) was 3.5 times as the voltage output slope (0.0018), well demonstrating the good sensitivity of power output signals, leading to better sensitivity of the PMMFC.

3.6. Shock significance analysis of PMMFC power outputs

The regression slopes after high concentration shocks (e.g. 20 mg/L Cr^{6+}, 10 mg/L Cr^{6+}, 200 mg/L NaClO, 100 mg/L NaClO and 200 mg/L NaAC) were 50–100 times higher than those before the shock (Table S2), indicating the sharp drop of the power output of PMMFCs after these shocks. In addition, the P values of the regression slope for these shocks were less than 10%, demonstrating that the drop of the power output was related with time. The

changes of the slopes and P values clearly distinguished the power output signals from noises. For the low concentration shocks (e. g. 5 mg/L Cr^{6+} and 50 mg/L NaClO), the regression slopes were similar to those before the shocks (Table S2), meaning that the low concentration shocks did not cause significant changes to the power outputs. The statistical regression analysis demonstrated that PMMFC sensors with the power outputs as signals can clearly distinguish the shock from the signal noise. The average coefficient variation (CV) of the power output of PMMFCs in the stable status (before shocks) was only 0.38 in all tests (data not shown), which was similar to previous membrane-based MFC sensors (CV: 0.44, Xu et al., 2015), indicating that the power output of PMMFCs in the stable status had the same pattern as the voltage output of MFCs.

3.7. Significance of PMMFCs for self-supported in situ monitoring "shocks" in wastewater

The unique bioelectrochemical feature of MFCs possesses a great potential for real-time monitoring shocks in wastewater. This study targeted at three imminent challenges (anode material, signal sensitivity, and operational sustainability) of MFC sensors by developing paper-based multi-anode configuration, utilizing the enlarged power output as sensor signal, and integrating MFC with PMS to self-support sensors. With filter paper as the biofilm supporter anode and carbon ink as the electron collector (as shown in Fig. S2), PMMFC enhanced the power output 8 times as CCMMFC. Multi-anode exhibited much higher power output than single anode. PMMFCs possessed distinct advantages: short startup duration (couple hours) and high power output steadily increasing with anode number. Using power output as the indicator is more sensitive than voltage output (clearly verified by high signal slopes), and thus substantially reducing the possibility of false warning. More importantly, the power simulation of PMS showed the capability of self-sustained data transmission, which can revolutionize on-line monitoring by effectively harvesting the power generated from multi-anode MFCs. The PMMFC integrated with PMS holds a great promise as a disposable self-sufficient real-time biosensor for general wastewater shock screening. With the good sensitivity and self-supported data transmission exhibited by 4-anode PMMFCs, power output can be further enhanced with more paper-based anodes packed (e.g. 8, 12), and an even better performance of PMMFC sensors would be expected.

Further works could be conducted to optimize the configuration of the PMMFC and enhance its long-term monitoring performance. First, the anode material (filter paper) tested in this study lasted for 2 months and showed a good mechanic strength. For long-term monitoring in wastewater (e.g. months and years), advanced material with high mechanic strength and electronic activity (e.g. nanopaper (Henriksson et al., 2008), nanoporous graphene membrane (Hauser and Schwerdtfeger, 2012)) should be developed. Nevertheless, the super low cost and the compact structure of PMMFCs make the routine replacement possible. Second, the carbon ink layer on the filter paper could be automatically coated using a printer rather than manually coating in this study, which will generate an evenly-distributed carbon layer, reduce R_{in} and energy loss, and ultimately achieve high sensitivity and accuracy for various shocks. Third, a quantitative correlation of power output and shock concentrations/types should be developed for PMMFC biosensors to validate the capability of real-time screening of shocks in wastewater.

4. Conclusion

Novel paper-based multi-anode microbial fuel cell (PMMFC) integrated with PMS was developed as a "self-sustained shock sensor" for real time in situ monitoring wastewater quality. Hydrophilic microporous paper-based anode coated with highly conductive carbon power accelerated bacterial adhesion and electron transfer. PMMFC exhibited much shorter acclimation duration (2–3 h) than traditional CCMMFC (3–15 days). With parallel anode connection, PMMFC enhanced the power output 6 times as CCMMFC, and 4 times as single anode MFC. Power output of PMMFC was more sensitive than voltage output under various shocks (heavy metal, disinfectant, and organic compound), verified by the power output slope 2.5–3.5 times as the voltage output. The statistical analysis of PMMFC signals showed that the regression slopes distinguished shock concentrations. The PMMFC integrated with PMS effectively enhanced the power output of parallel-connected multi-anode, possessed tight paper-packed structure, and achieved high sensitivity to a wide range of shocks.

Appendix A. Supplementary material

Supplementary data associated with this article can be found in the online version at http://dx.doi.org/10.1016/j.bios.2016.05.018.

References

Aelterman, P., Rabaey, K., Pham, H.T., Boon, N., Verstraete, W., 2006. Environ. Sci. Technol. 40 (10), 3388–3394.
Brungs, W.A., 1973. J. (Water Pollut. Control Fed.), 2180–2193.
Chang, I.S., Moon, H., Jang, J.K., Kim, B.H., 2005. Biosens. Bioelectron. 20 (9), 1856–1859.
Curtis, T.M., Widder, M.W., Brennan, L.M., Schwager, S.J., van der Schalie, W.H., Fey, J., Salazar, N., 2009. Lab Chip 9 (15), 2176–2183.
Donovan, C., Dewan, A., Heo, D., Beyenal, H., 2008. Environ. Sci. Technol. 42 (22), 8591–8596.
Donovan, C., Dewan, A., Peng, H., Heo, D., Beyenal, H., 2011. J. Power Sources 196 (3), 1171–1177.
Droppo G.W., Schienbein L.A., Harris B.E., Hammerstrom D.J., inventors. International Power System, Inc., assignee, 2003. United States patent US 6,628,011.
Dukan, S., Belkin, S., Touati, D., 1999. Arch. Biochem. Biophys. 367 (2), 311–316.
Fraiwan, A., Mukherjee, S., Sundermier, S., Lee, H.S., Choi, S., 2013. Biosens. Bioelectron. 49, 410–414.
Gupta, V.K., Gupta, M., Sharma, S., 2011. Water Res. 35 (5), 1125–1134.
Hauser, A.W., Schwerdtfeger, P., 2012. J. Phys. Chem. Lett. 3 (2), 209–213.
Henriksson, M., Berglund, L.A., Isaksson, P., Lindstrom, T., Nishino, T., 2008. Biomacromolecules 9 (6), 1579–1585.
Jiang, J., Zhao, Q., Wei, L., Wang, K., 2010. Water Res. 44 (7), 2163–2170.
Jouanneau, S., Recoules, L., Durand, M.J., Boukabache, A., Picot, V., Primault, Y., Lakel, A., Sengelin, M., Barillon, B., Thouand, G., 2014. Water Res. 49, 62–82.
Karra, U., Muto, E., Umaz, R., Kölln, M., Santoro, C., Wang, L., Li, B., 2014. Int. J. Hydrog. Energy 39 (36), 21847–21856.
Kim, M., Hyun, M.S., Gadd, G.M., Kim, H.J., 2007. J. Environ. Monit. 9 (12), 1323–1328.
Kolenbrander, P.E., Palmer, R.J., Periasamy, S., Jakubovics, N.S., 2010. Nat. Rev. Microbiol. 8 (7), 471–480.
Kumlanghan, A., Liu, J., Thavarungkul, P., Kanatharana, P., Mattiasson, B., 2007. Biosens. Bioelectron. 22 (12), 2939–2944.
Li, W.W., Yu, H.Q., He, Z., 2014. Energy Environ. Sci. 7 (3), 911–924.
Liu, B., Lei, Y., Li, B., 2014. Biosens. Bioelectron. 62, 308–314.
Liu, B., Williams, I., Li, Y., Wang, L., Bagtzoglou, A., McCutcheon, J., Li, B., 2016. Biosens. Bioelectron. 79, 435–441.
Liu, H., Logan, B.E., 2004. Environ. Sci. Technol. 38 (14), 4040–4046.
Liu, H., Cheng, S., Logan, B.E., 2005. Environ. Sci. Technol. 39 (14), 5488–5493.
Livak, K.J., Schmittgen, T.D., 2001. Methods 25 (4), 402–408.
Logan, B.E., 2009. Nat. Rev. Microbiol. 7 (5), 375–381.
Logan, B.E., Hamelers, B., Rozendal, R., Schröder, U., Keller, J., Freguia, S., Aelterman, P., Verstraete, W., Rabaey, K., 2006. Environ. Sci. Technol. 40 (17), 5181–5192.
McKenna, S.M., Davies, K.J.A., 1988. Biochem. J. 254 (3), 685–692.
Monser, L., Adhoum, N., 2002. Sep. Purif. Technol. 26 (2), 137–146.
Mukherjee, S., Su, S., Panmanee, W., Irvin, R.T., Hassett, D.J., Choi, S., 2013. Sens. Actuators A: Phys. 201, 532–537.
Nguyen, T.H., Fraiwan, A., Choi, S., 2014. Biosens. Bioelectron. 54, 640–649.
Oh, S., Logan, B.E., 2005. Water Res. 39 (19), 4673–4682.
Oh, S., Min, B., Logan, B.E., 2004. Environ. Sci. Technol. 38 (18), 4900–4904.
Okochi, M., Mima, K., Miyata, M., Shinozaki, Y., Haraguchi, S., Fujisawa, M., Kaneko, M., Masukata, T., Matsunaga, T., 2004. Biotechnol. Bioeng. 87 (7), 905–911.
Santoro, C., Agrios, A., Pasaogullari, U., Li, B., 2011. Int. J. Hydrog. energy 36 (20), 13096–13104.
Shantaram, A., Beyenal, H., Veluchamy, R.R., Lewandowski, Z., 2005. Environ. Sci. Technol. 39 (13), 5037–5042.
Shiers, D.W., Collinson, D.M., Kelly, N.J., Watling, H.R., 2016. Miner. Eng. 85, 55–65.
Stohs, S.J., Bagchi, D., 1995. Free Radic. Biol. Med. 18 (2), 321–336.

Tian, Y., Li, H., Li, L., Su, X., Lu, Y., Zuo, W., Zhang, J., 2015. Biosens. Bioelectron. 64, 189–195.
Wang, J., Zheng, Y., Jia, H., Zhang, H., 2014. Bioresour. Technol. 170, 483–490.
Wang, X., Gao, N., Zhou, Q., 2013. Biosens. Bioelectron. 43, 264–267.
Woznica, A., Nowak, A., Karczewski, J., Klis, C., Bernas, T., 2010. Chemosphere 81 (6), 767–772.
Xu, Z., Liu, B., Dong, Q., Lei, Y., Li, Y., Ren, J., McCutcheon, J., Li, B., 2015. Bioresour. Technol. 197, 244–251.
Yang, X.Y., Tian, G., Jiang, N., Su, B.L., 2012. Energy Environ. Sci. 5 (2), 5540–5563.
Zhang, L., Zhou, M., Wen, D., Bai, L., Lou, B., Dong, S., 2012. Biosens. Bioelectron. 35 (1), 155–159.
Zhou, M., 2015. Electroanalysis 27 (8), 1786–1810.
Zhou, M., Wang, J., 2012. Electroanalysis 24 (2), 197–209.